APPLIED AND ENVIRONMENTAL MICROBIOLOGY, June 2009, p. 4046–4052 Vol. 75, No. 12
0099-2240/09/$08.00+0 doi:10.1128/AEM.00247-09

Uncultivated Magnetotactic Cocci from Yuandadu Park in Beijing, China▽

Wei Lin[1,2] and Yongxin Pan[1]*

Bio-geomagnetism Group, Paleomagnetism and Geochronology Laboratory (SKL-LE), Institute of Geology and Geophysics, Chinese Academy of Sciences, Beijing 100029, China,[1] and Graduate University of Chinese Academy of Sciences, Beijing 100039, China[2]

Received 2 February 2009/Accepted 9 April 2009

In the present study, we investigated a group of uncultivated magnetotactic cocci, which was magnetically isolated from a freshwater pond in Beijing, China. Light and transmission electron microscopy showed that these cocci ranged from 1.5 to 2.5 μm and contained two to four chains of magnetite magnetosomes, which sometimes were partially disorganized. Overall, the size of the disorganized magnetosomes was significantly smaller than that arranged in chains. All characterized magnetosome crystals were elongated (shape factor = 0.64) and fall into the single-domain size range (30 to 115 nm). Comparative 16S rRNA gene sequence analysis and fluorescence in situ hybridization showed that the enriched bacteria were a virtually homogeneous population and represented a novel lineage in the *Alphaproteobacteria*. The closest cultivated relative was magnetotactic coccoid strain MC-1 (88% sequence identity). First-order reversal curve diagrams revealed that these cocci had relatively strong magnetic interactions compared to the single-chain magnetotactic bacteria. Low-temperature magnetic measurements showed that the Verwey transition of them was ~108 K, confirming magnetite magnetosomes, and the delta ratio δ_{FC}/δ_{ZFC} was >2. Based on the structure, phylogenetic position and magnetic properties, the enriched magnetotactic cocci of *Alphaproteobacteria* are provisionally named as "*Candidatus* Magnetococcus yuandaducum."

Magnetotactic bacteria (MTB) can mineralize intracellular nanosized iron oxides or sulfides called magnetosomes, which in most MTB are normally single-domain (SD) magnetite with a narrow range of grain sizes from 30 to 120 nm (3). The chain configuration of magnetosomes renders MTB able to navigate the oxic-anoxic interface in chemically stratified environments by swimming along the Earth's magnetic field (13). Diverse MTB, including coccoid, spirillar, rod-shaped bacteria and multicellular magnetotactic prokaryotes with one, two, or more chains of magnetosomes, thrive in a broad range of aquatic environments, which sometimes even are dominant strains of the microbial biomass in sediment (10, 47). Based on their phylogeny, all currently known MTB can be divided into two taxonomic groups: *Proteobacteria* and *Nitrospira* phyla (2).

When MTB die, the magnetosomes can be preserved in sediment as fossil magnetosomes (or magnetofossils) (6). Fossil magnetosomes have been found in lacustrine and deep-sea sediments (6, 35, 43, 51), which are stable carriers of natural remanence and may play substantial contributions to the bulk magnetization of sediments due to their SD sizes (6, 19, 26, 32, 33). Moreover, since most known MTB are microaerophilic or anaerobic and are concentrated in the oxic-anoxic transition zone, the presence and characteristics of MTB species in vertically stratified sediments can be used as a potential paleoenvironmental proxy (19, 44, 45). However, how to identify bacterial magnetite or greigite (Fe_3S_4) in sediments is still challenging. Recently, characterizing the magnetic properties of MTB has attracted increasing interests because magnetic techniques are fast and effective in distinguishing bacterial crystals from abiogenic magnetic minerals in sediments (11, 26, 27, 33, 38).

In spite of their wide distribution and abundance in aquatic environments, most MTB are intractable, and so far only a few of them, e.g., *Magnetospirillum gryphiswaldense* strain MSR-1 (41), *M. magnetotacticum* strain AMB-1 (17), *M. magnetotacticum* strain MS-1 (4), and magnetotactic coccoid strain MC-1 (24), can be grown in pure culture. Until recently, most insights into the molecular characterizations and magnetic properties of MTB have been based on pure cultures, which have a single magnetosome chain per cell (10, 11, 19, 20, 25, 27, 28, 37, 38, 42, 52). However, knowledge of uncultivated MTB, especially strains with multiple chains of magnetosomes that are commonly encountered in natural environments, remains limited. In the present study, we investigated a population of uncultivated magnetotactic cocci with multiple magnetosome chains, which were abundant in the pond in Yuan Dynasty Capital City Wall Relics Park (Yuandadu Park) in Beijing, China, in order to characterize their morphological features, phylogenetic positions, and magnetic properties and finally to classify them in a provisional *Candidatus* taxon.

MATERIALS AND METHODS

Sample and MTB collection. Surface sediments (3 to 5 cm) were collected by a shovel from a pond in Yuandadu Park and were divided into 600-ml plastic bottles covered with ~100 ml of pond water in the laboratory. The pH and temperature of sediments were 7.7 and 16.8°C, respectively. The "hanging-drop" method (14) was used to check the existence of MTB in samples. The south pole of a bar magnet was placed on the north side of a bottle near the water-sediment interface to enrich the MTB. After 1 h collection, MTB were removed from the

* Corresponding author. Mailing address: Paleomagnetism and Geochronology Laboratory, State Key Laboratory of Lithospheric Evolution, Institute of Geology and Geophysics, Chinese Academy of Sciences, 19 Bei Tu Cheng Xi Road, Beijing 100029, China. Phone: 86 (0)10 8299 8406. Fax: 86 (0)10 6237 2053. E-mail: yxpan@mail.iggcas.ac.cn.

▽ Published ahead of print on 17 April 2009.

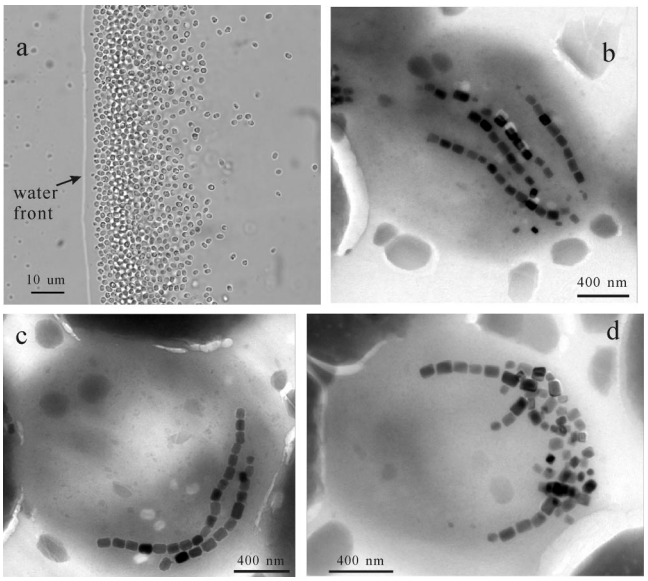

FIG. 1. Micrographs of enriched magnetotactic cocci as observed under a light microscope (a) and by TEM (b to d). Note that the applied field direction is from right to left in panel a. Chains of magnetosomes and disorganized magnetosomes coexist in panel d.

bottle by using a 5-ml Epperndorf pipette and further purified by using a double-ended open magnetic separation apparatus (22). The purified MTB cells were then washed with sterile distilled water twice and resuspended in 200 μl of sterile distilled water (~10^8 cells in total). About 20 μl of MTB enrichment was used for transmission electron microscopy (TEM) observation, 20 μl was used for phylogenetic analysis, 60 μl was used for fluorescence in situ hybridization, and the remaining 100 μl was used for magnetic measurements.

TEM observation. About 20 μl of MTB enrichment was deposited on Formvar-carbon-coated copper grids and allowed to air dry. Examination was performed with a FEI Tecnai 20 transmission electron microscope with an accelerating voltage of 120 kV. The length and width of magnetosomes were measured by using Adobe Photoshop. The sizes and the shape factor of the magnetosomes were calculated as (length + width)/2 and width/length, respectively.

Amplification of 16S rRNA genes, sequencing, and phylogenetic analysis. The bacterial universal primers 27F (5′-AGAGTTTGATCCTGGCTCAG-3′) and 1492R (5′-GGTTACCTTGTTACGACTT-3′) (5) were used to amplify 16S rRNA genes directly from the 20 μl of magnetically enriched MTB. PCR amplification and cloning procedures for construction of a 16S rRNA genes clone library were performed as previously reported (22, 23). Twenty clones were randomly picked up and subjected to sequencing.

Sequences retrieved in the present study were first checked for chimera formation with the CHECK_CHIMERA software of the Ribosomal Database Project II (RDP-II) (8). These sequences and their close relatives were then aligned using CLUSTAL W software (49) and corrected by manual inspection. A phylogenetic tree was subsequently constructed with MEGA version 4.0 (48) by using the neighbor-joining method. Bootstrap analysis for 100 replicates was performed for the estimation of reproducibility of tree topologies. Sequences acquired in the present study were deposited in the EMBL/GenBank/DDBJ databases under accession numbers FJ667777 and FJ667778.

Fluorescence in situ hybridization. Based on newly retrieved magnetotactic cocci sequences, an oligonucleotide probe, YDC69 (5′-CGCCAGCACCTTTC GGCCTGCTGC-3′, *Escherichia coli* 16S rRNA gene positions 69 to 92), was designed. The specificity was evaluated by using the PROBE_MATCH program in the RDP-II (8). The bacterial universal probe EUB338 (5′-GCTGCCTCCC GTAGGAGT-3′, positions 338 to 355, *E. coli* numbering) was used as a control (1). The probes YDC69 and EUB338 were synthesized and fluorescently labeled with hydrophilic sulfoindocyanine dye Cy3 and fluorescein phosphoramidite FAM at the 5′ ends, respectively, by Invitrogen.

Clones of *E. coli* with the inserted 16S rRNA genes of the uncultured *Magnetococcus* sp. clone 37 (22) was used as negative control. In situ hybridization was performed as described by Pernthaler et al. (34) at 46°C for 3 h in hybridization buffer with 20% (vol/vol) formamide. Then, 1 μl of probe (50 ng/μl) was mixed with 9 μl of hybridization buffer and then used for in situ hybridization. A fluorescence microscope (Olympus BX51) was used to record optical sections.

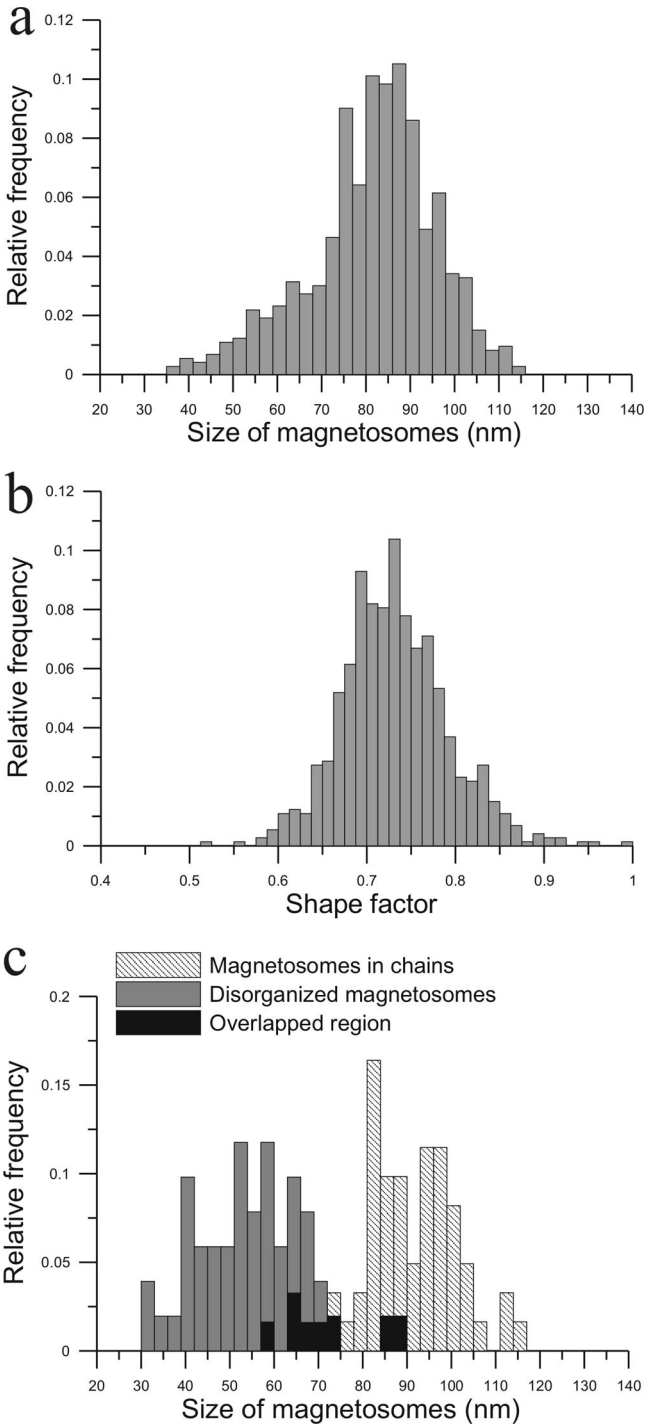

FIG. 2. (a to c) Histograms of size (a), shape factor of magnetosomes (b), and size distributions of magnetosomes in chains and disorganized magnetosomes (c) in enriched magnetotactic cocci.

Magnetic measurements of MTB. The 100-μl portion of MTB cells was placed in a nonmagnetic gelatin capsule, air dried overnight, and then used for magnetic measurements immediately. Hysteresis loop and the first-order reversal curve (FORC) analyses of the sample were measured on an alternating gradient force magnetometer (MicroMag 2900; Princeton Measurements Corp.). The hysteresis

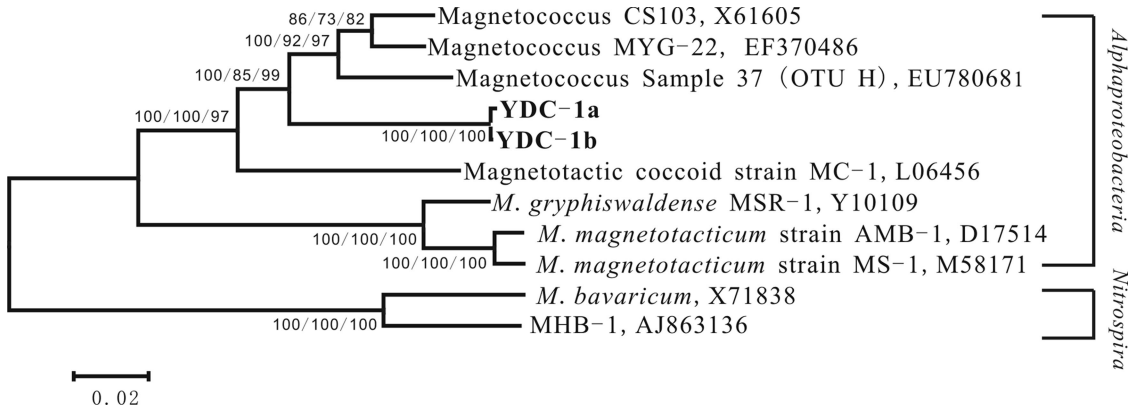

FIG. 3. Phylogenetic tree showing the relationship between the magnetotactic cocci and closely related magnetotactic bacteria. The tree is constructed based on neighbor-joining analysis. The sequences determined in the present study are indicated in boldface. Numbers at the nodes represent bootstrap values calculated by neighbor joining, maximum parsimony, and minimum evolution (100 times resampling analysis).

loop was measured at 0 to 1 T (1 T = 10^4 oersteds [Oe]), which yielded the saturation magnetization (M_s), saturation remanence (M_{rs}), and coercive force (B_c). The coercivity of remanence (B_{cr}) was acquired by measuring the back-field demagnetization curve by applying static field up to −300 mT. For FORC analysis, the MTB sample was first saturated in 1 T, and then the field was reversed to a number of negative fields and subsequently returned to the positive saturation. These processes generated a number of curves, which were then transformed into a FORC diagram. This diagram showed coercivity along the horizontal axis and magnetic interaction along the vertical axis (7).

Low-temperature magnetic characteristics were measured by using a quantum design magnetic property measurement system. The sample was first cooled to 5 K in a zero field environment and then saturated by applying a 2.5-T field. After being applied for 60 s, the field was removed, and the thermal demagnetization curve (zero field cooling [ZFC]) was measured from 5 to 300 K. The sample was then cooled from 300 to 5 K in the presence of a 2.5-T field. After the sample was kept at 5 K in a 2.5-T for 60 s, the field was turned off, and the thermal demagnetization curve (field cooling [FC]) was measured from 5 to 300 K. The Verwey transition temperature (T_v) was determined, at which the dM/dT is maximum (52). The delta ratio δ_{FC}/δ_{ZFC}, which was defined by Moskowitz et al. (27), was calculated from FC and ZFC data and could reflect the amount of remanence loss as warming through the Verwey transition. A δ_{FC}/δ_{ZFC} larger than 2 is considered to be an indicator of the presence of magnetite magnetosome chains of MTB.

RESULTS AND DISCUSSION

Morphology and magnetosome features. The magnetic enrichment of MTB was coccoid bacteria, size ranging from 1.5 to 2.5 μm (Fig. 1a). These cells contained 31 to 62 truncated hexahedral prisms of magnetosomes (Fig. 1b to d), which had an averaged length and width of 108 ± 32 nm and 69 ± 9 nm, respectively (n = 733). The size of magnetosome crystals varied from 30 to 115 nm and the averaged shape factor of them was 0.64, indicating stable SD crystals with marked elongation (Fig. 2a and b). Magnetosomes in these cells were usually arranged in 2 (31.6%), 3 (29.0%) and 4 (13.2%) chains (Fig. 1b and c). However, 11 of 42 characterized cells (26.2%) contained clustered magnetosomes adjacent to chains (Fig. 1d). Moreover, as seen in Fig. 2c, these disorganized magnetosomes were distinctly smaller than their counterparts aligned in chains.

One explanation for the existence of partially disorganized magnetosomes in the cocci is that the disorganized smaller magnetosomes are early-stage nonmature magnetosomes that may gradually form chains as they grow. If this is true, it implies that the mechanism involving in the spatial arrangement of magnetosomes in these bacteria may be different from that proposed for cultivated *Magnetospirillum* strains AMB-1 and MSR-1, where empty magnetosome vesicles first assembled into a chain structure with the help of particular proteins (e.g., MamK and MamJ), and then the magnetite crystals start to biomineralize in the chain-arranged vesicles (18, 42). Alternatively, we cannot exclude the possibility that the empty magnetosome vesicles are aligned into multiple chains, whereas the formation of magnetosomes occurs randomly, therefore the small crystals are not apparently aligned. A third possibility is that the Yuandadu cells with distinctly different magnetosome arrangements are from different sediment depths and hence reflect different environmental conditions (e.g., the concentration of O_2), since these magnetotactic cocci are magnetically enriched from bulk sediments that would not conserve the stratified structure of the original habitat (9). Fourth, many transposase genes are located within the magnetosome island in cultivated *Magnetospirillum* strain MSR-1 (15, 50), which frequently results in spontaneous rearrangements or deletions of magnetosome genes and causes the bacteria to mutate during cultivation in the laboratory (10). Similarly, we assume that magnetotactic cocci with disorganized chains may undergo mutation in the environment. The last possibility is perhaps due to the preparation of the sample for TEM observation; the fact that the cells were air dried that may have caused considerably shrinking and disorganized partial chains.

Phylogenetic analysis and in situ hybridization. Nearly complete 16S rRNA genes of magnetically enriched MTB were amplified and cloned. Twenty clones were randomly chosen for partial sequencing (>800 bp, covering the four variable regions V1 to V4). All of them showed high similarity (>99%), and two clones were subsequently fully bidirectionally sequenced (YDC-1a and YDC-1b). The similarity between them was 99.7%. These sequences were compared to the NCBI nucleotide database by using the BLAST algorithm; they were found to affiliate with the *Alphaproteobacteria* and had a maximum identity of 91.1% with uncultured *Magnetococcus* sp. clone 37 (22) (Fig. 3). The closest cultivated relative was marine magnetotactic coccoid strain MC-1, although the sequence similar-

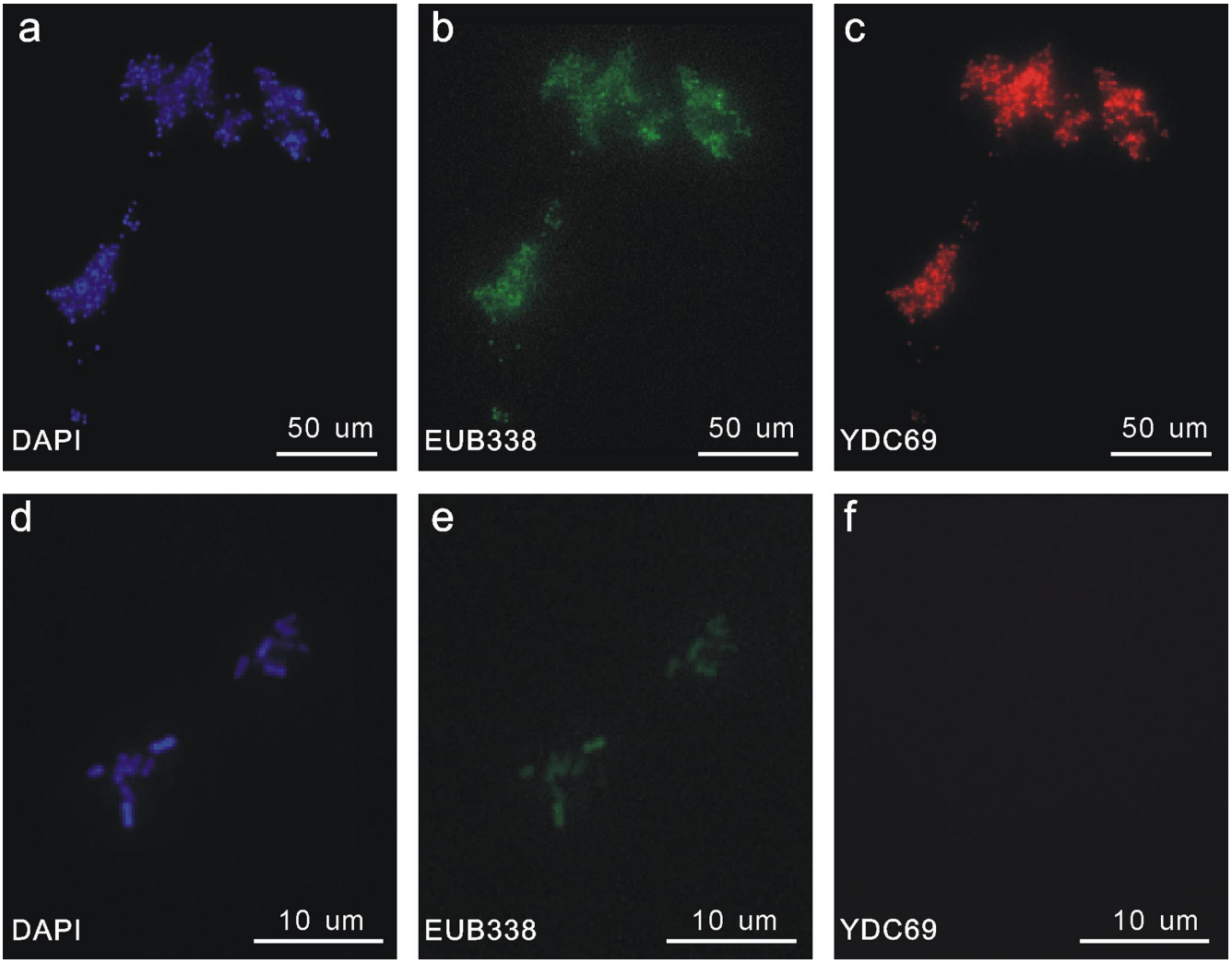

FIG. 4. In situ hybridization of magnetically enriched coccoid cells (a to c) and negative control of clones of *E. coli* with the inserted 16S rRNA genes of the uncultured *Magnetococcus* sp. clone 37 (d to f). In panels a to c, the same microscopic field is shown after staining with DAPI (a), after hybridization with 5′-FAM-labeled bacterial universal probe EUB338 (b), and after hybridization with 5′-Cy3-labeled probe YDC69 specific for magnetotactic cocci (c). In panels d to f, the same microscopic field is shown in after staining with DAPI (d), after hybridization with 5′-FAM-labeled bacterial universal probe EUB338 (e), and after hybridization with 5′-Cy3-labeled probe YDC69 (f).

ity was rather low (88%) (24). To confirm that the sequences obtained here originated truly from the enriched cocci, a specific oligonucleotide probe, YDC69, was designed to be complementary to the retrieved sequences and applied to in situ hybridization of enriched MTB cells. Comparative sequence analysis using the PROBE_MATCH function in RDP-II showed that the probe YDC69 had at least two mismatches with all other 16S rRNA genes. Fluorescence microscopy revealed a strong signal for all collected cocci after hybridization with the bacterial universal probe EUB338 and the specific probe YDC69 (Fig. 4a, b, and c), whereas clones of *E. coli* with insertions of 16S rRNA genes of the uncultured *Magnetococcus* sp. clone 37 could not be hybridized by the specific probe YDC69 (Fig. 4d, e, and f). These results suggested that the enriched magnetotactic cocci were a homogeneous population since they could be specifically hybridized with the probe YDC69.

In spite of a homogeneous taxonomic population, we note that the number of magnetosome chains in cells changed from two to four. This indicates that no strict correlation exists between magnetosome arrangements and phylogenetic positions of magnetotactic cocci (9, 46). In other words, the number of magnetosome chains is not suitable as a phenotypic criterion for distinguishing the taxonomy of MTB.

Freshwater sediments often harbor diverse groups of MTB, including cocci, spirilla, rods, and vibrios (12, 22, 46). However, only one homogeneous taxonomic population was found in the fresh sediment of Yuandadu Park. It was previously suggested that the competitive interactions within bacteria might shape a dominant diversity pattern observed in particular locations (53). Therefore, the magnetotactic cocci observed here may outperform other kinds of MTB through competition in the pond. On the other hand, several environmental factors, such as habitat type and habitat heterogeneity, can play roles in selecting the specific population of bacteria (16). It was reported by Pan et al. (31) that a single population of ovoid-coccoid MTB was dom-

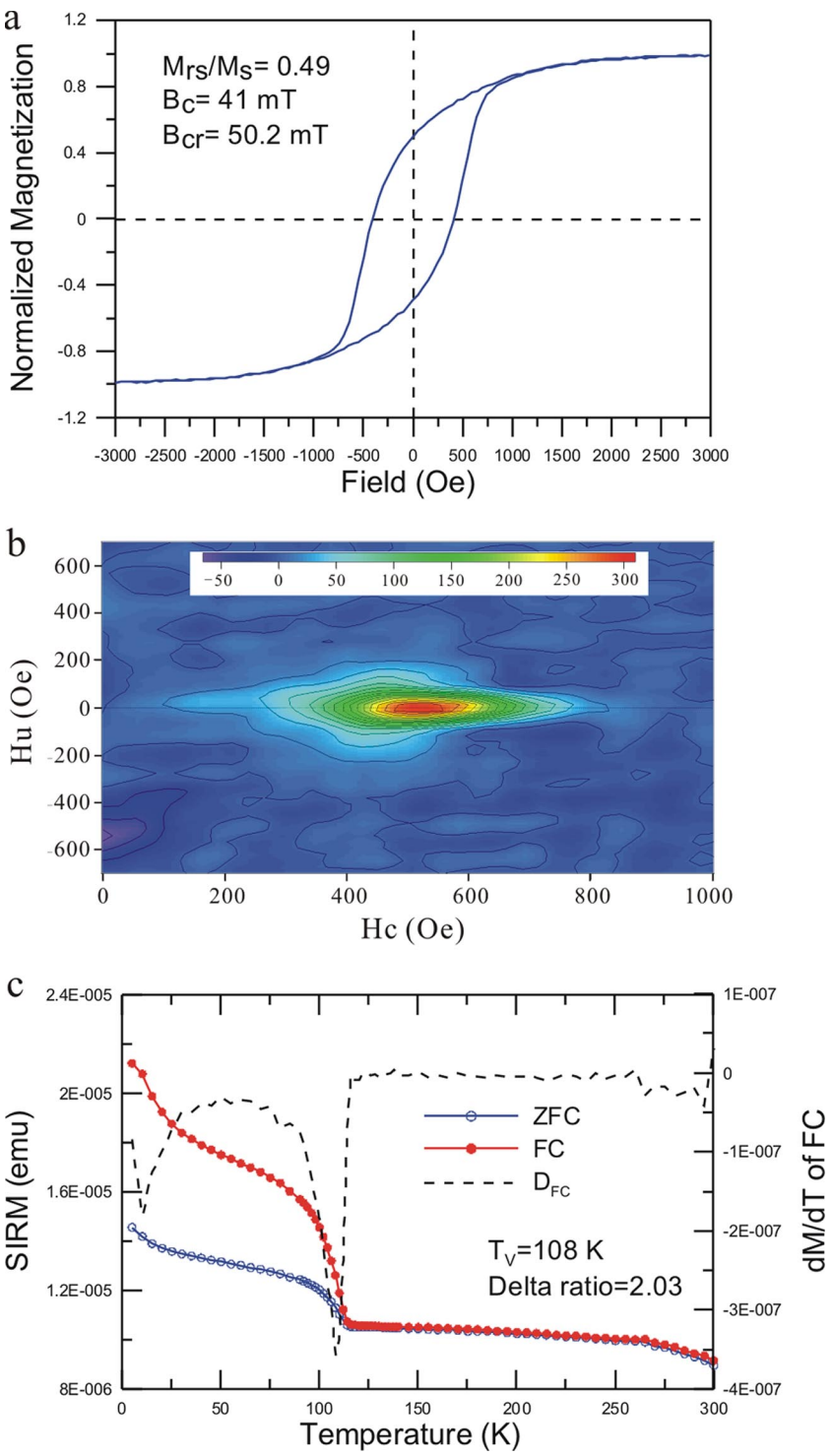

FIG. 5. (a to c) Room temperature hysteresis loop (a) and FORC diagram (b) and low-temperature demagnetization behaviors (c) of the enriched magnetotactic cocci. M_s, M_{rs}, B_c, and B_{cr} represent the saturation magnetization, saturation remanence, coercive force, and coercivity of remanence, respectively. The smoothing factor of FORC diagram is 4. D_{FC}, the first derivatives of the FC curve (dashed line). T_V, the Verwey transition temperature.

inant in the low tide zone of the East China Sea near Qingdao due to the specific habitat selection. This may be true for our sample as well. The sediments in the Yuandadu pond are from time to time exposed to air because of pumping and irrigation (two to three times per year). Another possibility is that, due to the intrinsic limitations of magnetic collection procedure (23), other kinds of MTB, which exist in the sediment, may be missed during the magnetic enrichment process.

Magnetic characteristics. A room temperature hysteresis loop of the cocci was a pot-bellied shape and closed at a field of ~150 mT (Fig. 5a). The values of the coercivity (B_c) and the coercivity of remanence (B_{cr}) were 41 and 50.2 mT, respectively. They have a remanence ratio M_{rs}/M_s of 0.49 and a coercity ratio B_{cr}/B_c of 1.22. The FORC diagram spread and closed along the $H_c = 0$ axis, with a relative narrow distribution along the H_u axis (Fig. 5b). The characteristic interaction field $H_{b1/2}$, as defined by the value of the interaction field at half maximum of FORC distribution (39), is 5.3 mT. Clearly, both the hysteresis loop and the FORC diagram of the magnetotactic cocci indicate that their magnetosomes are stable SD particles, which is consistent with crystal sizes observed by TEM (Fig. 2a) (33, 36, 40).

The FORC diagram is able to reflect the chain-chain interactions, the intrachain interactions (particle-particle interaction within a chain), and cell-cell interactions (7, 33). The vertical spread of FORC contours ($H_{b1/2}$ = 5.3 mT) in the present study is comparable to that of multiple-chain MTB reported previously ($H_{b1/2}$ = 6.3 mT) (33) but more prominent than that of single-chain AMB-1 ($H_{b1/2}$ = 2.4 mT) (21). This indicates that the magnetotactic cocci with multiple chains and partially disorganized magnetosomes have stronger magnetic interactions within cells than the MTB with only single chains. One thing that should be noted is that the B_c (41 mT) and B_{cr} (50.2 mT) for the coccus samples are much higher than the corresponding values reported for other MTB samples (11, 21, 25, 27, 33, 37, 38). Although the multiple-chain structures and disorganized magnetosomes may increase magnetic interaction and tend to reduce coercivity, we attribute the higher coercivity values to the elongated magnetosome crystals (the average shape factor is 0.64) in the cocci. The advantage of high coercivity is apparent since it can stabilize the net magnetic dipole moment of magnetosome chains and thus benefit the orientation of these north-seeking cocci.

The FC and ZFC curves of coccoid cells were shown in Fig. 5c. Saturation isothermal remanent magnetization on both FC and ZFC curves significantly decreased by ~108 K during the Verwey transition of magnetite. The transition temperature is similar to observed T_v for other MTB strains with magnetite magnetsosomes (86 to 117 K). The observed lower T_v for the magnetosome magnetite compared to that of the stoichiometric magnetite (120 to 125 K) (37, 38) has been interpreted as nonstoichiometry of bacterial magnetite (26, 33).

Moskowitz et al. (27) first proposed that a δ_{FC}/δ_{ZFC} ratio greater than 2 can be a detection criterion for bacterial magnetite based on cultivated MTB strains MV-1 and MV-2 and *M. magnetotacticum* strain MS-1. The validity of the Moskowitz test has been further proved by other cultivated and uncultivated MTB (26, 33, 37, 52). Recently, Li et al. (21) found that *M. magnetotacticum* strain AMB-1, which produces three to five segmental chains (subchains) of magnetosome, passed the test as well. We observed that the δ_{FC}/δ_{ZFC} of cocci with multiple chains and partially disorganized magnetosomes is also greater than 2 (2.03). Therefore, we propose that the Moskowitz test, along with other rock magnetic parameters, is a powerful and fast tool for the detection of magnetite magnetosomes from environmental samples.

Description of "*Candidatus* Magnetococcus yuandaducum." Based on the recommendations of Murray and Schleifer (29) and Murray and Stackebrandt (30), the sequence-based potential new microorganisms could be recorded by a "*Candidatus*" designation. The magnetotactic cocci enriched in the present study are designated "*Candidatus* Magnetococcus yuandaducum." The bacteria are magnetically collected from freshwater pond sediment. The cells are coccoid, with an average diameter between 1.5 to 2.5 μm. They contain 31 to 62 truncated hexahedral prisms of magnetite magnetosomes (shape factor, 0.64), which are arranged into two to four chains per cell that sometimes appear partially disorganized. The cells are north-seeking MTB with a motility speed of ~112 μm/s under 4 Oe magnetic fields (data not shown). The coercivity, the vertical spread of FORC contours ($H_{b1/2}$), the Verwey transition temperature, and the corresponding delta ratio are 41 mT, 5.3 mT, 108 K, and 2.03, respectively. The bacteria belong to a new genus within the *Alphaproteobacteria*. The assignment is based on the 16S rRNA gene sequence, on GenBank accession numbers FJ667777 and FJ667778, and on the 16S rRNA-targeted oligonucleotide probe YDC69 (5′-CGCCAGCACCTTTCGG CCTGCTGC-3′). The organism has yet to be cultivated.

ACKNOWLEDGMENTS

We thank Caicai Liu for help with FORC measurements, Jinhua Li for the electron microscopy observations, and Qingsong Liu for useful discussions. We are grateful to two anonymous reviewers for their valuable comments.

This study was supported by NSFC grants 40821091 and 40325011. Y.P. acknowledges the financial support of the CAS "100 Talents" program.

REFERENCES

1. **Amann, R., L. Krumholz, and D. A. Stahl.** 1990. Fluorescent-oligonucleotide probing of whole cells for determinative, phylogenetic, and environmental studies in microbiology. J. Bacteriol. **172:**762–770.
2. **Amann, R., J. Peplies, and D. Schüler.** 2006. Diversity and taxonomy of magnetotactic bacteria. Springer, Berlin, Germany.
3. **Bazylinski, D. A., and R. B. Frankel.** 2004. Magnetosome formation in prokaryotes. Nat. Rev. Microbiol. **2:**217–230.
4. **Blakemore, R. P., D. Maratea, and R. S. Wolfe.** 1979. Isolation and pure culture of a freshwater magnetic spirillum in chemically defined medium. J. Bacteriol. **140:**720–729.
5. **Brandl, M. T., B. Quinones, and S. E. Lindow.** 2001. Heterogeneous transcription of an indoleacetic acid biosynthetic gene in *Erwinia herbicola* on plant surfaces. Proc. Natl. Acad. Sci. USA **98:**3454–3459.
6. **Chang, S. B. R., and J. L. Kirschvink.** 1989. Magnetofossils, the magnetization of sediments, and the evolution of magnetite biomineralization. Annu. Rev. Earth Planet. Sci. **17:**169–195.
7. **Chen, A. P., R. Egli, and B. M. Moskowitz.** 2007. First-order reversal curve (FORC) diagrams of natural and cultured biogenic magnetic particles. J. Geophys. Res. doi:10.1029/2006JB004575.
8. **Cole, J. R., B. Chai, T. L. Marsh, R. J. Farris, Q. Wang, S. A. Kulam, S. Chandra, D. M. McGarrell, T. M. Schmidt, G. M. Garrity, and J. M. Tiedje.** 2003. The Ribosomal Database Project (RDP-II): previewing a new autoaligner that allows regular updates and the new prokaryotic taxonomy. Nucleic Acids Res. **31:**442–443.
9. **Cox, B. L., R. Popa, D. A. Bazylinski, B. Lanoil, S. Douglas, A. Belz, D. L. Engler, and K. H. Nealson.** 2002. Organization and elemental analysis of P-, S-, and Fe-rich inclusions in a population of freshwater magnetococci. Geomicrobiol. J. **19:**387–406.
10. **Faivre, D., and D. Schüler.** 2008. Magnetotactic bacteria and magnetosomes. Chem. Rev. **108:**4875–4898.
11. **Fischer, H., G. Mastrogiacomo, J. F. Loffler, R. J. Warthmann, P. G. Weidler, and A. U. Gehring.** 2008. Ferromagnetic resonance and magnetic characteristics of intact magnetosome chains in *Magnetospirillum gryphiswaldense*. Earth Planet. Sci. Lett. **270:**200–208.
12. **Flies, C. B., J. Peplies, and D. Schüler.** 2005. Combined approach for characterization of uncultivated magnetotactic bacteria from various aquatic environments. Appl. Environ. Microbiol. **71:**2723–2731.
13. **Frankel, R. B., D. A. Bazylinski, M. S. Johnson, and B. L. Taylor.** 1997. Magneto-aerotaxis in marine coccoid bacteria. Biophys. J. **73:**994–1000.
14. **Greenberg, M., K. Canter, I. Mahler, and A. Tornheim.** 2005. Observation of magnetoreceptive behavior in a multicellular magnetotactic prokaryote in higher than geomagnetic fields. Biophys. J. **88:**1496–1499.

15. **Grünberg, K., E. C. Muller, A. Otto, R. Reszka, D. Linder, M. Kube, R. Reinhardt, and D. Schüler.** 2004. Biochemical and proteomic analysis of the magnetosome membrane in *Magnetospirillum gryphiswaldense*. Appl. Environ. Microbiol. **70:**1040–1050.
16. **Horner-Devine, M. C., K. M. Carney, and B. J. M. Bohannan.** 2004. An ecological perspective on bacterial biodiversity. Proc. R. Soc. Lond. Ser. B Biol. Sci. **271:**113–122.
17. **Kawaguchi, R., J. G. Burgess, and T. Matsunaga.** 1992. Phylogeny and 16S rRNA sequence of *Magnetospirillum* sp. AMB-1, an aerobic magnetic bacterium. Nucleic Acids Res. **20:**1140.
18. **Komeili, A.** 2007. Molecular mechanisms of magnetosome formation. Annu. Rev. Biochem. **76:**27.1–27.16.
19. **Kopp, R. E., and J. L. Kirschvink.** 2008. The identification and biogeochemical interpretation of fossil magnetotactic bacteria. Earth Sci. Rev. **86:**42–61.
20. **Kopp, R. E., B. P. Weiss, A. C. Maloof, H. Vali, C. Z. Nash, and J. L. Kirschvink.** 2006. Chains, clumps, and strings: magnetofossil taphonomy with ferromagnetic resonance spectroscopy Earth Planet. Sci. Lett. **247:** 10–25.
21. **Li, J., Y. Pan, G. Chen, Q. Liu, L. Tian, and W. Lin.** 2009. Magnetite magnetosome and fragmental chain formation of *Magnetospirillum magneticum* AMB-1: transmission electron microscopy and magnetic observations. Geophys. J. Int. **177:**33–42.
22. **Lin, W., J. Li, D. Schüler, C. Jogler, and Y. Pan.** 2009. Diversity analysis of magnetotactic bacteria in Lake Miyun, northern China, by restriction fragment length polymorphism. Syst. Appl. Microbiol. doi:10.1016/j.syapm.2008.10.005.
23. **Lin, W., L. Tian, J. Li, and Y. Pan.** 2008. Does capillary racetrack-based enrichment reflect the diversity of uncultivated magnetotactic cocci in environmental samples? FEMS Microbiol. Lett. **279:**202–206.
24. **Meldrum, F., S. Mann, B. R. Heywood, R. B. Frankel, and D. A. Bazylinski.** 1993. Electron microscopy study of magnetosomes in a cultured coccoid magnetotactic bacterium. Proc. R. Soc. Lond. B **251:**231–236.
25. **Moskowitz, B. M.** 1988. Magnetic properties of magnetotactic bacteria. J. Magn. Magn. Mater. **73:**273–288.
26. **Moskowitz, B. M., D. A. Bazylinski, R. Egli, R. B. Frankel, and K. J. Edwards.** 2008. Magnetic properties of marine magnetotactic bacteria in a seasonally stratified coastal pond (Salt Pond, MA, USA). Geophys. J. Int. **174:**75–92.
27. **Moskowitz, B. M., R. B. Frankel, and D. A. Bazylinski.** 1993. Rock magnetic criteria for the detection of biogenic magnetite. Earth Planet. Sci. Lett. **120:**283–300.
28. **Moskowitz, B. M., R. B. Frankel, D. A. Bazylinski, H. W. Jannasch, and D. R. Lovley.** 1989. A comparison of magnetite particles produced anaerobically by magnetotactic and dissimilatory iron-reducing bacteria. Geophys. Res. Lett. **16:**665–668.
29. **Murray, R. G. E., and K. H. Schleifer.** 1994. Taxonomic notes: a proposal for recording the properties of putative taxa of prokaryotes. Int. J. Syst. Bacteriol. **44:**174–176.
30. **Murray, R. G. E., and E. Stackebrandt.** 1995. Taxonomic note: implementation of the provisional status *Candidatus* for incompletely described prokaryotes. Int. J. Syst. Bacteriol. **45:**186–187.
31. **Pan, H. M., K. L. Zhu, T. Song, K. Yu-Zhang, C. Lefevre, S. Xing, M. Liu, S. J. Zhao, T. Xiao, and L. F. Wu.** 2008. Characterization of a homogeneous taxonomic group of marine magnetotactic cocci within a low tide zone in the China Sea. Environ. Microbiol. **10:**1158–1164.
32. **Pan, Y., N. Petersen, A. Davila, L. Zhang, M. Winklhofer, Q. Liu, M. Hanzlik, and R. Zhu.** 2005. The detection of bacterial magnetite in recent sediments of Lake Chiemsee (southern Germany). Earth Planet. Sci. Lett. **232:**109–123.
33. **Pan, Y., N. Petersen, M. Winklhofer, A. Davila, Q. Liu, T. Frederichs, M. Hanzlik, and R. Zhu.** 2005. Rock magnetic properties of uncultured magnetotactic bacteria. Earth Planet. Sci. Lett. **237:**311–325.
34. **Pernthaler, J., F. O. Glockner, W. Schonhuber, and R. Amann.** 2001. Fluorescence in situ hybridization (FISH) with rRNA-targeted oligonucleotide probes. Methods Microbiol. **30:**207–226.
35. **Petersen, N., T. von Dobeneck, and H. Vali.** 1986. Fossil bacterial magnetite in deep-sea sediments from the South Atlantic Ocean. Nature **320:**611–615.
36. **Pike, C. R., A. P. Roberts, and K. L. Verosub.** 2001. First-order reversal curve diagrams and thermal relaxation effects in magnetic particles. Geophys. J. Int. **145:**721–730.
37. **Pósfai, M., B. M. Moskowitz, B. Arato, D. Schüler, C. Flies, D. A. Bazylinski, and R. B. Frankel.** 2006. Properties of intracellular magnetite crystals produced by *Desulfovibrio magneticus* strain RS-1. Earth Planet. Sci. Lett. **249:** 444–455.
38. **Prozorov, R., T. Prozorov, S. K. Mallapragada, B. Narasimhan, T. J. Williams, and D. A. Bazylinski.** 2007. Magnetic irreversibility and the Verwey transition in nanocrystalline bacterial magnetite. Phys. Rev. B doi:10.1103/PhysRevB.76.054406.
39. **Roberts, A. P., Q. S. Liu, C. J. Rowan, L. Chang, C. Carvallo, J. Torrent, and C. S. Horng.** 2006. Characterization of hematite (α-Fe_2O_3), goethite (α-FeOOH), greigite (Fe_3S_4), and pyrrhotite (Fe_7S_8) using first-order reversal curve diagrams. J. Geophys. Res. doi:10.1029/2006JB004715.
40. **Roberts, A. P., C. R. Pike, and K. L. Verosub.** 2000. First-order reversal curve diagrams: a new tool for characterizing the magnetic properties of natural samples. J. Geophys. Res. Solid Earth **105:**28461–28475.
41. **Schleifer, K. H., D. Schüler, S. Spring, M. Weizenegger, R. Amann, W. Ludwig, and M. Kohler.** 1991. The genus *Magnetospirillum* gen. nov. description of *Magnetospirillum gryphiswaldense* sp. nov. and transfer of *Aquaspirillum magnetotacticum* to *Magnetospirillum magnetotacticum* comb. nov. Syst. Appl. Microbiol. **14:**379–385.
42. **Schüler, D.** 2008. Genetics and cell biology of magnetosome formation in magnetotactic bacteria. FEMS Microbiol. Rev. **32:**654–672.
43. **Schumann, D., T. D. Raub, R. E. Kopp, J. L. Guerquin-Kern, T. D. Wu, I. Rouiller, A. Smirnov, S. K. Sears, U. Lücken, S. M. Tikoo, R. Hesse, J. L. Kirschvink, and H. Vali.** 2008. Gigantism in unique biogenic magnetite at the Paleocene-Eocene thermal maximum. Proc. Natl. Acad. Sci. USA doi:10.1073/pnas.0803634105.
44. **Snowball, I., P. Sandgren, and G. Petterson.** 1999. The mineral magnetic properties of an annually laminated Holocene lake-sediment sequence in northern Sweden. Holocene **9:**353–362.
45. **Snowball, I., L. Zillen, and P. Sandgren.** 2002. Bacterial magnetite in Swedish varved lake-sediments: a potential bio-marker of environmental change. Quat. Int. **88:**13–19.
46. **Spring, S., R. Amann, W. Ludwig, K.-H. Schleifer, D. Schüler, K. Poralla, and N. Petersen.** 1994. Phylogenetic analysis of uncultured magnetotactic bacteria from the alpha-subclass of *Proteobacteria*. Syst. Appl. Microbiol. **17:**501–508.
47. **Spring, S., R. Amann, W. Ludwig, K. H. Schleifer, H. van Gemerden, and N. Petersen.** 1993. Dominating role of an unusual magnetotactic bacterium in the microaerobic zone of a freshwater sediment. Appl. Environ. Microbiol. **59:**2397–2403.
48. **Tamura, K., J. Dudley, M. Nei, and S. Kumar.** 2007. MEGA4: molecular evolutionary genetics analysis (MEGA) software version 4.0. Mol. Biol. Evol. **24:**1596–1599.
49. **Thompson, J. D., D. G. Higgins, and T. J. Gibson.** 1994. CLUSTAL W: improving the sensitivity of progressive multiple sequence alignment through sequence weighting, positions-specific gap penalties and weight matrix choice. Nucleic Acids Res. **22:**4673–4680.
50. **Ullrich, S., M. Kube, S. Schubbe, R. Reinhardt, and D. Schüler.** 2005. A hypervariable 130-kilobase genomic region of *Magnetospirillum gryphiswaldense* comprises a magnetosome island which undergoes frequent rearrangements during stationary growth. J. Bacteriol. **187:**7176–7184.
51. **Vali, H., O. Forster, G. Amarantidis, and N. Petersen.** 1987. Magnetotactic bacteria and their magnetofossils in sediments. Earth Planet. Sci. Lett. **86:** 389–400.
52. **Weiss, B., S. Kim, J. Kirschvink, R. Kopp, M. Sankaran, A. Kobayashi, and A. Komeili.** 2004. Ferromagnetic resonance and low-temperature magnetic tests for biogenic magnetite. Earth Planet. Sci. Lett. **224:**73–89.
53. **Zhou, J. Z., B. C. Xia, D. S. Treves, L. Y. Wu, T. L. Marsh, R. V. O'Neill, A. V. Palumbo, and J. M. Tiedje.** 2002. Spatial and resource factors influencing high microbial diversity in soil. Appl. Environ. Microbiol. **68:**326–334.